

# System Component Degradation: Filter Clogging in a UAV Fuel System

Zakwan Skaf<sup>1</sup>, Omer F. Eker<sup>2</sup>, and Ian K. Jennions<sup>3</sup>

<sup>1,3</sup>*IVHM Centre, Cranfield University, UK*

*z.skaf@cranfield.ac.uk*  
*i.jennions@cranfield.ac.uk*

<sup>2</sup>*Artis Technology Systems, Turkey*  
*Omer.Eker@artesis.com*

## ABSTRACT

The filtration of possible contaminant is an essential part of many engineering processes in industry. Clogging of the filtration medium is one of the primary failure modes in many application areas leading to reduced performance and efficiency. Imitation of real life clogging scenarios in laboratory conditions is not an easy task to perform, but is demonstrated here, with the profiles obtained being injected into a fuel system rig. This paper shows generic results from two benchmark rigs. One is a fuel system laboratory test-bed representing an Unmanned Aerial Vehicle (UAV) fuel system and its associated electrical power supply, control system and sensing capabilities. It is specifically designed in order to replicate a number of component degradation faults with a high degree of accuracy and repeatability. The second is a purpose built filter clogging rig designed to give quality results to aid the development of prognostic algorithms. This paper's contribution is to show results from the filter clogging rig and derive a transfer function, the relationship between filter clogging pressures and the fuel system valve openings, to enable the fuel system rig to operate as if the clogging filter were part of the system. The results show that the local pressure drop obtained from the fuel rig can be made to closely match the pressure drop levels from the filter clogging rig. This opens up examination of the effects of filter clogging on the full fuel rig system, providing data for future system prognostic work.

## 1. INTRODUCTION

Integrated Vehicle Health Management (IVHM) provides an essential role in aircraft operation management, and continues to offer the potential for a paradigm shift in the way that aircraft organisations conduct business operations (Jennions, 2011). Benedettini et al. (2009) postulate that IVHM is also potentially applicable to non-vehicle systems such as industrial process plants and power generation

plants. While IVHM enables many disciplines with an integrated framework, the one current technology that promises the greatest gain is prognostics; it is fundamental to a number of service offerings, including Condition Based Maintenance (CBM). While prognostics has been successfully applied at the component level (Eker et al, 2016), application at the systems level is required and a step towards this is made in this paper.

Prognostics requires identification of the current health level and extrapolation to a predefined failure threshold, resulting in the estimation of remaining useful life (RUL). The output of prognostics (i.e. RUL) is the duration between the current time and the time at which the forecasted health level reaches a predefined threshold. The benefit of prognostics enables researchers and industry to reduce costs, and increase safety and availability, via better maintenance planning. In contrast with traditional maintenance philosophies, the IVHM approach enables modelling and tracking of individual equipment deterioration leading to a maintenance action only when it is necessary rather than performing scheduled maintenance. This all pre-supposes that data, of the right quality and quantity, is available. As this is sometimes lacking, an approach utilising benchtop experimentation is implemented here.

The failure mechanism of system components is often a gradual degradation process. Therefore, system component degradation data can provide information for assessing the reliability and estimating the RUL of system components. In some cases, actual degradation can be observed with time. An example of this would be a crack growing with time. As the crack grows to a critical length the component will fail. On the other hand, some actual degradation processes are slow or cannot readily be observed. In these cases it may be possible to detect the deteriorating performance of the component or system. In addition, the lack of historical run-to-failure datasets available and insufficient instrumentation for measuring degradation are other reasons for doing

further benchmark tests, as presented here. It is also often useful to accelerate testing to increase the degradation rate to collect useful data in a reasonable time for prognosis. The implementation of accelerated degradation testing is an appropriate choice to overcome some of the obstacles in developing prognostics techniques in engineering, such as insufficient data, time and cost constraints.

The filtration phenomenon is of interest to several engineering industries including automotive, chemical, reactor, and process engineering applications. Several industrial applications such as food, petroleum, pharmaceuticals, metal production, and minerals embrace filtration processes (Sparks, 2011). The aim of the filtration system is to keep the rest of the system running smoothly, as well as keeping the process operational. Modern commercial vehicles and automobiles have numerous types of filters for fluids including fuel, lubricant, and intake air (Sutherland, 2010).

Fuel filters filtrate dirt and other contaminants in the fuel system such as sulphates, polymers, paint chips, dust, and rust particulates which are released from a fuel tank due to moisture or other numerous types of dirt that have been uplifted via a supply tanker (Wilfong et al., 2010, Jones, 2008). Consequences like engine and pump performance degradation due to increased abrasion and inefficient burning in the engine are the main motivators for fuel filtration, leading to a purified fuel. However, filtering the fuel brings with it some complications (e.g. clogging of filters). System flow rate and engine performance decline once a fuel filter is clogged. Jones (2008) reports that filter clogging indication due to fuel contamination may result in an aircraft having to return to the ground or divert for further fuel filter inspection or replacement. In today's maintenance planning, fuel filters are replaced or cleansed on a regular basis. Jones (2008) again reports that the Boeing 777 fuel filter inspections are performed every 2000 flight hours. Monitoring and implementation of prognostics on filtration system have the potential to avoid costs and increase safety by continuously monitoring the filters and only indicate maintenance when needed.

The clogging process of different types of filtration mechanisms has been studied in the literature. Roussel et al. (2007) presented a particle level filtration case study, stating that the general clogging process can be considered as a function of: ratio of particle to mesh pore size, solid fraction, and the number of grains arriving at each mesh hole during one test. Pontikakis et al. (2001) developed a mathematical model for dynamic behaviour of the filtering process for ceramic foam filters. The model is capable of estimation of the filtration efficiency, accumulation of particle mass in the filter, and the pressure drop throughout the filter. Roychoudhury et al. (2013) presented a diagnostic and prognostic solution for a water recycling system for next generation spacecraft. They simulated several failure

scenarios including clogging of membranes and filters. Baraldi et al. (2013), and Baraldi et al. (2015) developed a similarity-based and Gaussian process regression prognostic approach to estimate the remaining useful life (RUL) of sea water filters. Saarela et al. (2014) presented a nuclear research reactor air filter pressure drop modelling scheme which utilised gamma processes.

In this paper, the clogging filter phenomena will be simulated in the laboratory using two test rigs. The first rig is a fuel system rig, capable of emulating a number of degradation features in a highly controlled manner. The second rig (filter clogging rig), provides the degradation profile of the filter, created by running accelerated tests. This clogging profile is then injected into the fuel system rig to enable system prognostics to be explored.

The paper proceeds by presenting a brief description of both the fuel system rig and the filter clogging rig. Then, data collection from the filter clogging rig and its insertion into the fuel rig, to give realistic clogging profiles, is described. Finally, some conclusions are drawn and future work suggested.

**2. FUEL SYSTEM TEST RIG**

The fuel system test rig is a laboratory test-bed representing an Unmanned Aerial Vehicle (UAV) fuel system and its associated electrical power supply, control system and sensing capabilities (Niculita et al, 2014). It is specifically designed in order to replicate a number of component degradation faults with high accuracy and repeatability so that it can produce benchmark datasets to evaluate and assess algorithms. A schematic of the rig is shown in Figure 1 and a photograph of the physical rig in Figure 2.

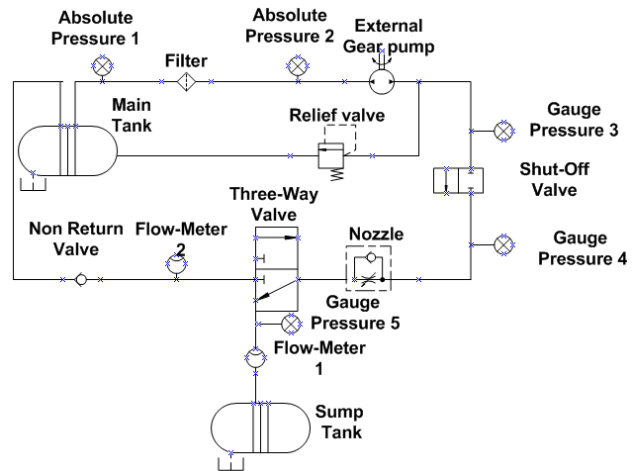


Figure. 1. Schematic of the Fuel System Rig

Fuel is replaced by water as the working fluid in the rig, and it is pumped by a gear pump around the circuit, which

contains a number of control valves. Referring to Figures 1 and 2, fluid is taken from the main tank through a filter before entering the gear pump. A back flow loop is controlled by a relief valve, while the main line proceeds through a shut off valve and a nozzle followed by a three-way valve. These, in combination, simulate flow being delivered to an engine; here the flow is simply put into the sump tank. The main loop concludes by the fluid passing through a non-return valve and returning to the main tank. Pressures and flow are measured at the points shown.

The rig enables injection of 5 fault modes via Direct Proportional Valves (DPVs), shown by the red circles in Figure 2. These valves can be closed very accurately and provide an ideal way of injecting repeatable faults into the rig. The faults considered are:

1. Clogging filter. The Filter is replaced by a DPV.
2. Degraded pump. The relief valve is replaced by a DPV enabling the flow to the rest of the rig to be controlled as if the pump was malfunctioning.
3. Stuck valve. The shut off valve is replaced by a DPV.
4. Leaking pipe. A DPV is used in conjunction with the 3 way valve to control leakage.
5. Clogged Nozzle. The nozzle is replaced by a DPV.

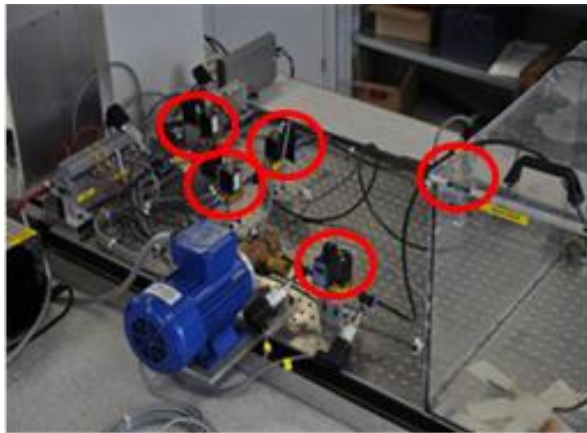


Figure 2. Fuel system test rig

In order to control and acquire data from the fuel system test rig, a system using National Instruments (NI) LabVIEW has been utilized. A CDAQ – 9172 device with six compact DAQ modules: NI 9485, NI 9205, NI 9472, NI 9401 and two NI 9263s is used. The NI 9485 is an 8-channel solid-state relay sourcing or sinking digital output module for any CompactDAQ or CompactRIO chassis. One channel was used to provide access to a solid-state relay for switching the

24V voltage applied to the shut-off valve in order to control the open/close position. The NI 9205 module receives the analogue voltage output from the pressure transducers and flow-meters, converts this information using the pre-defined calibration curves into digitized information readable on the GUI. The NI 9472 module is an 8-channel 24V logic, sourcing digital output module which provides the signals to the pump inverter in order to implement the pump controls. The NI 9401 module counts the rotational speed by taking the laser sensor analogue output pulses and converting them into frequency. The NI 9263 module has 4-channels, working at 100 kS/s, simultaneously updating the analogue output module which enables the implementation of the DPV position control. Valve position is modified by varying the voltage applied to the solenoid.

The main GUI is shown in Figure 3, where the controls are structured in three layers:

- The top layer contains the Pump Control Unit and the Valve Control Unit.
- The second layer enables control of the fault injection mechanisms at the component level. This is done via knobs that are setting the position of the five DPVs.
- The third layer allows injection of sensor faults (not discussed here).

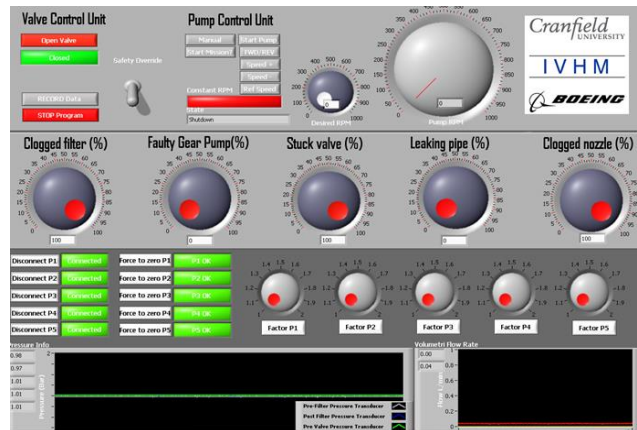


Figure 3. Fuel system – GUI for controls

The data presented to the user at the bottom of the GUI is:

- Pressures at different points of the system, like those shown in Figure 4.
- Volumetric flow rate in the main line.

In this work, we focus on the clogging filter failure mode, shown in Figure 4. The DPV is set to be initially fully open to capture the healthy scenario. By gradually closing the

DPV (progressing right to left), the clogging of the filter is replicated and the pressure responds accordingly. While this figure shows the response to closing the DPV, it is not representative of the progression of the real clogging process, input that will be taken from the filter clogging rig, discussed next.

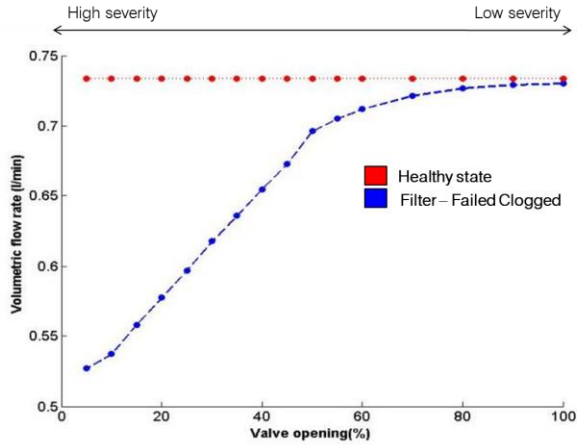


Figure 4. Physical behaviour – Clogged filter scenario

### 3. FILTER CLOGGING RIG

An experimental rig was developed by Eker et al (2016) to investigate the physics of filter clogging and the ability of hybrid prognostic methods to predict it. A schematic of the rig is shown in Figure 5 and a photograph in Figure 6. The rig works by a pump moving a suspension of finely graded particles through a filter, on each side of which pressure is measured. The pressure drop over time, supplemented by camera images, characterise the clogging process.

The major components in the system are:

- Pump: there are different types of pump enabling a liquid to flow through a complex system. Since the system here involves contaminants in the fluid, a peristaltic pump has been used as its mechanism will not interfere with the particles in the liquid. A Masterflex® SN-77921-70 peristaltic pump was installed in the system to maintain the flow of the prepared suspension. The pump is a positive displacement source, providing a flow rate ranging from 0.28 to 1700 ml/min.
- Dampener: rigid tubing is used in most of the rig to prevent any unwanted tube expansion due to pressure build up. A Masterflex® pulse dampener is installed on the downstream side of pump to eliminate any pressure pulsations in flow.
- Tank: one half-sphere-shaped main tank and two subsidiary tanks (i.e. reservoir tank and clean water tank) are installed in the system. The sphere shape tank bowl enables the stirrer to work efficiently

leading to homogeneously distributed slurry in the tank. The clean water tank is used to fill-up the system components with clean water prior to each test, and eliminate bubbles. A Kern® 10000-1N type high precision weighing scale is placed under the reservoir tank to measure the slurry used.

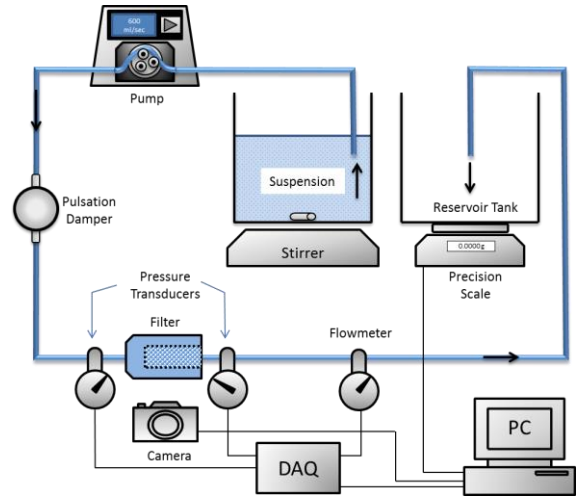


Figure 5. Schematic of filter clogging rig

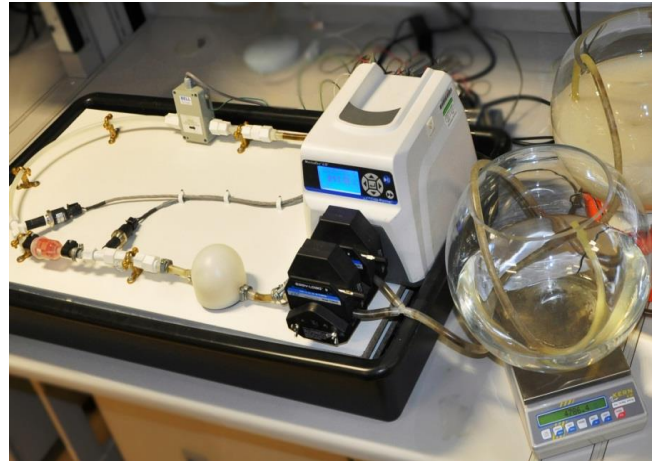


Figure 6. Filter clogging rig

- Particles: the suspension is composed of Polyetheretherketone (PEEK) particles and water. PEEK particles have a density (1.3g/cm<sup>3</sup>) close to that of room temperature water and have a low water absorption level. The particles have a wide size distribution as seen in Figure 7. For this reason, narrowing the distribution by sieving is

found to be necessary before conducting experiments.

- Camera: A high quality macro lens camera is positioned over the filter chamber, to take macro pictures every two seconds. The mesh inside the filter, and the retained particles, can be clearly captured. Pressure and flow rate data are combined with some of the image data to form a complete data package for each particle size and flow rate tested.

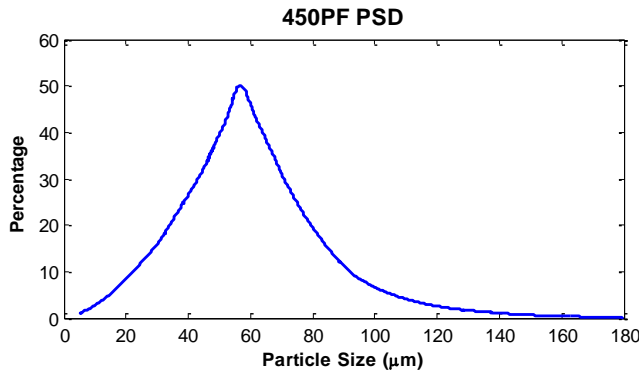


Figure 7. PEEK particle size distribution

**4. EXPERIMENT AND RESULTS**

This section presents the results from the accelerated filter clogging experiments. It then shows how these can be used to obtain a transfer function expressing the pressure drop in the filter clogging rig as a valve closing angle for the fuel system rig, for general use in the fuel system rig.

**4.1 Data collection from the filter clogging rig**

The PEEK particles, whose size distribution are shown in Figure 7, are procured in powder form. As there is a wide range of particle sizes, from 5 to 180 microns, wet sieving is employed to narrow the particle size range into 3 categories as shown in Table 1. The non-sieved particles are used as a fourth, reference, case.

It is crucial to maintain the operational and environmental conditions consistent for the subset of data being considered and care is taken with the experiments to ensure this. For each particle size, four different flow rates were explored, giving different solid ratios, each of which was repeated a number of times to ensure accuracy. The entire dataset is comprised of 56 run-to-failure accelerated aging experiments.

The fuel filters chosen for this experiment are the 125 micron pore sized Baldwin® BF7725 type, shown below in Figure 8.

Table 1. Operational profiles

Profile No.	Particle Size (µm)	Solid Ratio (%)	Sample Size
1	45-53	0.4	4
2		0.425	4
3		0.45	4
4		0.475	4
5	53-63	0.4	4
6		0.425	4
7		0.45	4
8		0.475	4
9	63-75	0.4	4
10		0.425	4
11		0.45	4
12		0.475	4
13	Non-sieved	0.4	2
14		0.425	2
15		0.45	2
16		0.475	2

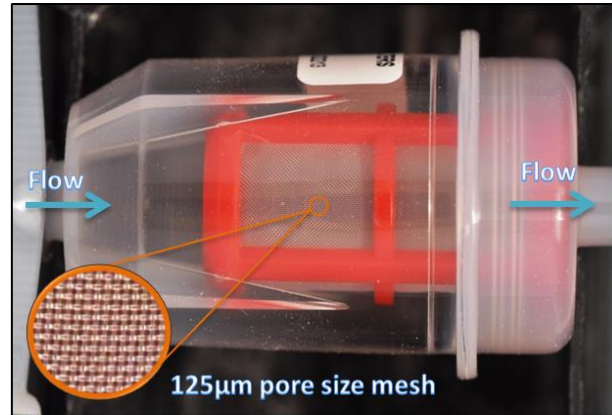


Figure 8. Baldwin fuel filter

Pressure and flow rate readings, the main indicators of clogging, have been collected continuously. Each clogging experiment has been run and monitored until the filter has clogged, which is judged to have happened when 15 psi is recorded across the filter.

Data collection is conducted with an NI DAQ-9203 16 bit analogue current output module, which is connected to an NI cDAQ-9174 4-slot USB chassis. The sampling rate is adjusted to 100Hz within the LabVIEW environment, which is sufficient to capture the pulses generated by the pump. For visualisation purposes, data is low pass filtered and down-sampled to 1Hz as displayed in Figure 9. Each trajectory in the figure represents differential pressure profiles for each distinct run-to-failure experiment. As seen

from the figure the variation in the profiles is small, although discernible, at the beginning of the clogging phenomena. However, the spread in the dataset increases as the experiment nears to the end of life. Variation in the experimental results reflects the variation in the sixteen different operational profiles.

Figure 9 shows the entire dataset for all 56 experimental runs. In the figure, the red scale trajectories represent the experiments under the first four operational profiles where particle size varies from 45 to 53 microns. Similarly, green and cyan coloured curves pertain to the 53-63 and 63-75 micron band of the distribution. Finally, the blue line trajectories obtained with non-sieved (i.e. original) particles. The lighter colour scales, within each separate colour, correspond to lower solid ratios. As seen in the figure, the experiments conducted with lower solid ratios take longer to reach end of life compared to the higher solid ratio experiments.

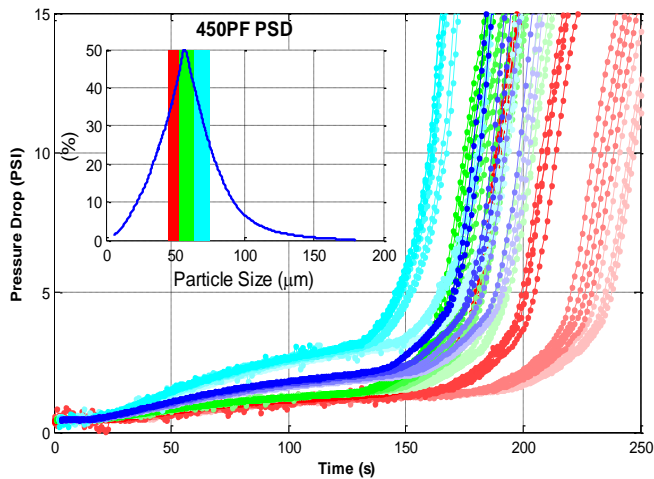


Figure 9. Summary of Filter Clogging Experimental Data

#### 4.2 Calibration of the fuel system rig

As the degradation phenomena of the filter in the fuel system is emulated by closing the DPV, there is a need to obtain a transfer function that converts the pressure drop across the filter from the filter clogging rig into valve opening rate as a function of time. In the fuel system rig, the valve is completely opened when there is no clogging in the filter and completely closed when the filter is clogged.

The conversion of pressure drop values into valve opening rate could be considered physically, but it was known that the DPV closure effect on the fuel rig was non-linear and hence the following 3 step process was used:

Step 1. Assume that the DPV opening is directly proportional to the pressure drop by:

$$VOR_t = VOR_{max}(1 - \Delta P_t / \Delta P_{max}) \quad (1)$$

where:

$VOR_t$  : Valve opening at time 't'

$VOR_{max}$  : Maximum valve opening (taken as 100%)

$\Delta P_t$  : Pressure drop at time 't'

$\Delta P_{max}$  : Pressure drop threshold (taken as 10psi because it is the maximum pressure drop which can be obtained from the fuel system rig)

Taking Profile 4 from Table 1, computing the DPV positions from equation 1, and applying them to the fuel rig, gives the results shown in Figure 10. Clearly there is a mismatch in pressure drop that needs to be adjusted.

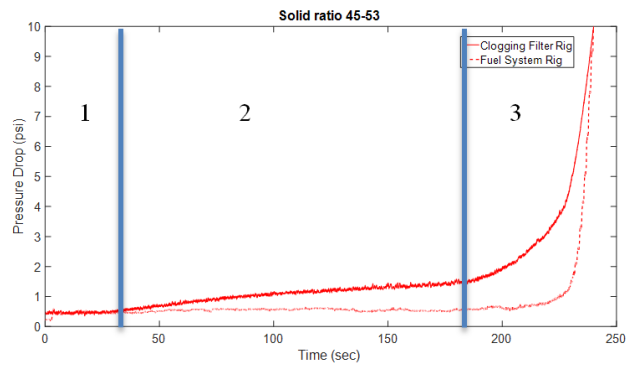


Figure 10. Pressure drop data comparison

The pressure drop across the filter from the filter clogging rig can be divided into three stages, as shown in Figure 10. In the first stage the pressure drop remains relatively constant (in the range  $0 < t < 43$ ). In the second stage, the pressure drop increases steadily (in the range  $43 < t < 183$ ). In the final stage (when  $t > 183$ ), the pressure drop enters an exponentially growing region. In contrast, the pressure drop across the valve from the fuel system rig shows two stages. During the first stage (in the range  $0 < t < 17$ ) the pressure drop remains relatively constant. In the second stage (when  $t > 17$ ), the pressure drop values are exponential.

By taking profiles 4, 8 and 12 from Table 1, computing the DPV positions from equation 1, and applying them to the fuel rig, the results shown in Figure 11 are obtained. The solid and dashed lines in Figure 11 represent the pressure drop across the filter from the filter clogging rig and the fuel system rig, respectively, at different operation condition. The blue line represents the pressure drop when the particle size varies from 45 to 53 micron. Similarly, the green line pertains to the 53-63 micron band of the distribution. Finally, the red line trajectory is obtained when the particle size varies between 63 and 75 micron.

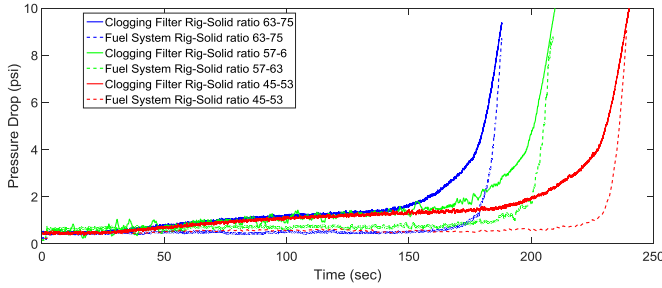


Figure 11. Pressure drop data comparison at different operational profiles

The root mean squared error (RMSE) is one of the most commonly used accuracy metrics for time series analysis, and is used here to assess the accuracy of the transfer function. RMSE values are calculated by:

$$RMSE = \sqrt{\frac{\sum_{i=1}^n (y_i - f_i)^2}{n}} \quad (2)$$

Where:

- $y_i$  : Filter clogging rig pressure drop at time point 'i'
- $f_i$  : Fuel system pressure drop at time point 'i'
- $n$  : Number of time intervals taken

In this way, values of RMSE are calculated and given in the table below:

Table 2. Accuracy measure for samples

Particle Size (µm)	RMSE
45-53	0.958
53-63	1.003
63-75	1.189

From Table 2 we can conclude that RMSE increases when the size of the particles increase. Also, the values of RMSE for 45-53 and 53-63 are very close, while the values of RMSE for the 63-75 particle size are relatively large. The smaller values of RMSE indicate a better match between the pressure drop across the filter from the filter clogging rig and the fuel system rig. Table 2 shows that the overall value of the RMSE is relatively high, which means the error is big, reflecting the discrepancy seen in Figure 11. In other words, large RMSE values reflect the assumption's poor ability to accurately represent the relationship between the valve opening and pressure drop across the filter.

Step 2. While the first assumption (equation 1) was to consider the valve opening proportional to the pressure drop, physically it seems that it may be better expressed as proportional to the Reynolds number:

$$Re = \frac{\text{inertial forces}}{\text{viscous forces}} = \frac{\rho u L}{\mu} \quad (3)$$

where:

- $\rho$  is the density of the fluid
- $u$  is the velocity of the fluid
- $L$  is a characteristic linear dimension
- $\mu$  is the viscosity of the fluid

As the fluid properties are the same in both rigs this would indicate scaling on velocity, or the square root of pressure, as indicated by:

$$VOR_t = VOR_{max} (1 - (\Delta P_t / \Delta P_{max})^{0.5}) \quad (4)$$

For profile 12, with particles size variation between 63 and 75 micron, both the original DPV settings and the modified valve openings are shown in Figure 12.

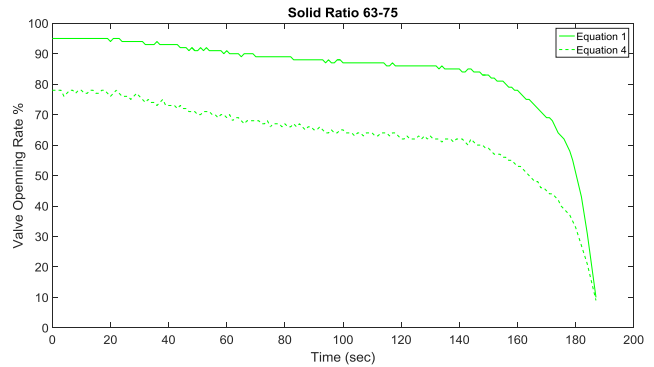


Figure 12. Original and Modified Valve Openings

The seeming discrepancy at time=0 can be explained as follows. There is a small pressure drop across the filter at the beginning of the filter clogging phenomena due to the resistance the filter gives to the flow. For a given value of this pressure drop,  $\Delta P_t / \Delta P_{max}$ , equation (1) will yield a larger valve opening than equation (4) due to the presence of the square root in the latter formula.

Step 3. Applying the new valve opening (equation 4) to Profiles 4, 8 and 12 from Table 1 gives Figure 13, showing good agreement between the pressure drop in the filter clogging rig and in the fuel system rig at different operation condition.

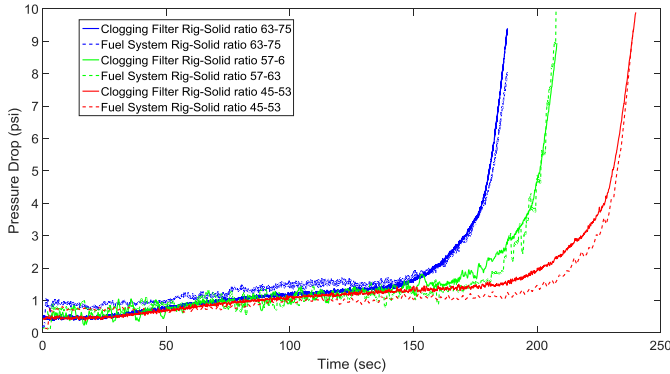


Figure 13. Pressure drop data comparison at different operational profiles

In a similar manner to Table 2, Table 3 summaries the RMSE values resulting from the use of equation 4 as the transfer function. The values of RMSE for 45-53, 53-63 are again very close, while the values of RMSE for the 63-75 particle size are now smaller, the overall trend from Table 2 having reversed. Also, the values of RMSE are much smaller in Step 3 compared with the previous values in Step 1. This result means that equation 4 represents a much more accurate relationship between the valve opening and the pressure drop across the filter in the fuel system rig.

Table 3. Accuracy measure for samples

Particle Size (µm)	RMSE
45-53	0.3407
53-63	0.3319
63-75	0.2877

5. CONCLUSION AND FUTURE WORK

In this work, the pressure drop associated with accelerated degradation of filter clogging are found from a stand-alone rig. These pressure profiles are then transferred into a fuel rig system so that filter clogging can be examined at the system level. The way in which the pressure drop is transferred is detailed and the transfer function described.

The pressure drop across a filter in the filter clogging rig is emulated by controlling the opening rate of the DPV in the fuel rig system, as a function of time. The pressure drop results from both rigs, once the valve transfer function is established, are in good agreement. This is further emphasized by computing the RMSE index, which verifies the effectiveness of the proposed method for different operational profile.

This work will continue to look at system level prognostics, both experimentally and theoretically, by considering

degradation profiles of different fuel system components and predicting the lifetime of the system in which these components interact.

ACKNOWLEDGEMENT

This research was supported by the IVHM Centre, Cranfield University, UK, and its industrial partners.

REFERENCES

Baraldi, P., Di Maio, F., Mangili, F. and Zio, E. (2013). A belief function theory method for prognostics in clogging filters, *Chemical Engineering Transactions*, vol. 33, pp. 847-852.

Baraldi, P., Mangili, F. and Zio, E. (2015), A prognostics approach to nuclear component degradation modelling based on Gaussian Process Regression, *Progress in Nuclear Energy*, vol. 78, no. 0, pp. 141-154.

Benedettini, O., Baines, T. S., Lightfoot, H. W. and Greenough, R. M. (2009), State-of-the-art in integrated vehicle health management, *Proceedings of the Institution of Mechanical Engineers, Part G: Journal of Aerospace Engineering*, vol. 223, no. 2, pp. 157-170.

Endo, Y., Chen, D.-R., and Pui, D. Y. H. (1998), Effects of Particle Polydispersity and Shape Factor During Dust Cake Loading on Air Filters, *Powder Technol.*, 98(3):241-249

Eker, Omer F., Camci, Fathi, Jennions, Ian K., 2016, Physics-based Modelling of Filter Clogging Phenomena, *Mechanical Systems and Signal Processing* 75, pp 395-412.

Jennions, I. K. (2011), *Integrated Vehicle Health Management: Perspectives on an Emerging Field*, SAE International.

Jones, M. (2008), Engine Fuel Filter Contamination, QTR\_03 ed., Boeing AeroMagazine.

NASA (Oct. 1992), Research and technology goals and objectives for Integrated Vehicle Health Management (IVHM), report NASA-CR-192656.

Niculita, Octavian, Skaf, Zakwan, Jennions, Ian K., 2014, The Application of Bayesian Change Point Detection in UAV Fuel Systems, 3rd International Conference on Through-Life Engineering Services, *Procedia CIRP* 22 pp115-121, 7 pages.

Pontikakis, G. N., Koltsakis, G. C. and Stamatelos, A. M. (2001), Dynamic filtration modeling in foam filters for diesel exhaust, *Chemical Engineering Communications*, vol. 188, pp. 21-46.

Roussel, N., Nguyen, T. L. H. and Coussot, P. (2007), General probabilistic approach to the filtration process, *Physical Review Letters*, vol. 98, no. 11.

Roychoudhury, I., Hafiyhuk, V. and Goebel, K. (2013), Model-based diagnosis and prognosis of a water recycling system, *IEEE Aerospace Conference*, 2013, pp. 1-9.

- Saarela, O., Hulsund, J. E., Taipale, A. and Hegle, M. (2014), Remaining Useful Life Estimation for Air Filters at a Nuclear Power Plant, *2nd International Conference of the Prognostics and Health Management Society*.
- Sparks, T. (2011), *Solid-Liquid Filtration: A User's Guide to Minimizing Cost & Environmental Impact, Maximizing Quality & Productivity*, First Edition ed, Elsevier Science & Technology Books.
- Sutherland, K. (2010), Mechanical engineering: The role of filtration in the machinery manufacturing industry, *Filtration and Separation*, vol. 47, no. 3, pp. 24-27.
- Wilfong, D., Dallas, A., Yang, C., Johnson, P., Viswanathan, K., Madsen, M., Tucker, B. and Hacker, J. (2010), Emerging challenges of fuel filtration, *Filtration*, vol. 10, no. 2, pp. 107-117.



**Prof. Ian Jennions** is Director of the IVHM Centre at Cranfield University. He has over 30 years of industrial experience working in engineering and service. He has led the development and growth of the Centre, in research and education, over the last six years and currently contributes to the 15 active projects. The Centre has offered a short course in IVHM every year since it opened, and the world's first IVHM MSc in 2011. Ian is a member of the Health Management and Prognostics NTC, he is on the editorial Board for the International Journal of Condition Monitoring, a Director of the PHM Society, contributing member of the SAE IVHM Steering Group and HM-1 IVHM committee, and a Fellow of IMechE, RAeS and ASME. He is the editor of four books on IVHM for SAE.

## Biographies



**Dr. Zakwan Skaf** is the Course Director of the Integrated Vehicle Health Management (IVHM) short course and Module Leader of Diagnostics and Prognostics for the MSc Through-life System Sustainment course at Cranfield University. Zakwan received the B.S. degree from the faculty of Mechanical Engineering in 2001, and the MSc and Ph.D. degrees from the University of Manchester, Control Systems Centre, Manchester, U.K., in 2006 and 2011 respectively. He has worked in different projects on aerospace and automotive applications before his current role as research fellow in prognostics and diagnostics at the IVHM Centre. Research interests are in a broad range of aspects related to health management system and controls engineering.



**Dr. Omer F. Eker** works as the product and business development manager in Artesis Technology Systems based in Gebze Technology Park, Turkey. He previously worked as a post-doctorate research fellow in IVHM Centre, Cranfield University, and holds his PhD from the School of Aerospace Transport and Manufacturing, Cranfield University, UK. He received his BS in Mathematics and MS in Computer Science. He was involved in a project on physical network modelling of the environmental control system of a specific passenger aircraft. He was also involved in various projects funded by the UK and Turkish governments and/or industrial bodies in between 2009 - 2014. His research interests include fault diagnostics and prognostics, predictive maintenance, condition monitoring, pattern recognition, artificial intelligence, and machine learning.